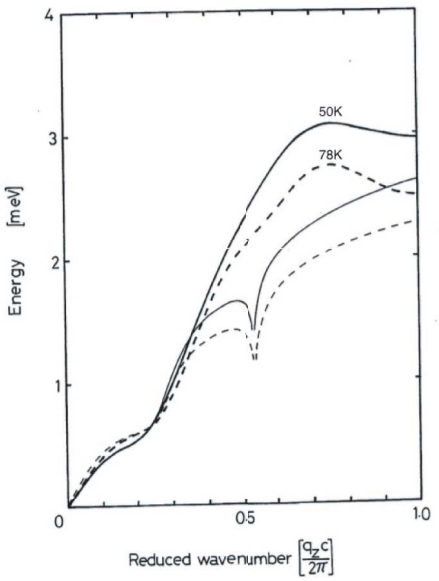

Fig. 16. Magnon dispersions of helical Holmium along the c direction: Full curves at 50 K, and broken curves at 78 K; Thick curves for the experiment and thin curves for the theory.

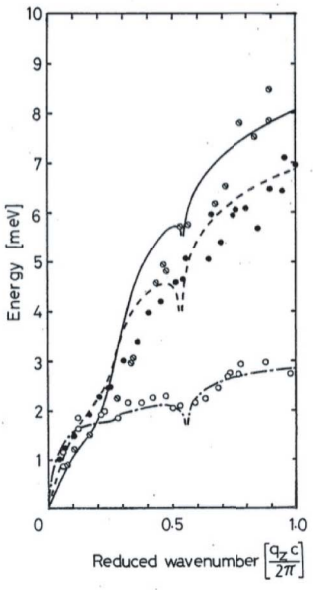

Fig. 17. Magnon dispersions along the c axis of helical phases of Tb_xY_{1-x} alloys at 4.7 K. Experiments: ○, $x = 0.1$; ●, $x = 0.5$; ⊖, $x = 0.76$. Theory: Chain curve, $x = 0.1$; broken curve, $x = 0.5$; full curve, $x = 0.76$.

Table 2. Fitting parameters J_0 and B with values of ± errors for helical Ho.

T [K]	J_0 [meV]	B [meV]
78	$2.54\ ^{+0.31}_{-0.11}$	$0.0369\ ^{-0.0040}_{+0.0017}$
50	$3.02\ ^{+0.31}_{-0.11}$	$0.0346\ ^{-0.0051}_{+0.0067}$

Table 3. Fitting parameters J_0 and B for the magnon dispersions of $Tb_{1-x}Y_x$ alloys.

x	J_0 [meV]	B [meV]
0.1	1.88	0.312
0.5	6.59	0.337
0.75	8.27	0.314

Using the above model parameters and two parameters J_0 and B, we can calculate the magnon dispersion for helical Ho. The parameters J_0 and B are chosen so as to be the mean absolute difference between those two dispersions for $q_z < 0.35\ [2\pi/c]$ less than 0.05 meV. Table 2 gives the values for J_0 and B with the values of errors. Figure 16 shows the comparison between the calculated dispersions and the experimental dispersions [14].

The most prominent feature that the magnon energies for $q_z < Q$ increase with increasing temperature is explained by the temperature dependence of $\Delta = \sigma\Delta_0$, that is, the non-linear effect of the c-f exchange interaction. The effective axial-anisotropy constant in Table 1 is consistent with the values estimated above [1] but its temperature dependence is too weak.

Thirdly let us consider the magnon dispersions in the helical phases of Tb_xY_{1-x} alloys ($0.05 < x < 0.85$) whose moments are confined in the c plane [35] (see Fig. 17). When the mean-field-approximation is applied to those alloys, the magnon dispersion is given by Eq. (73), provided that S is replaced by xS.

For Tb the model parameter $\tilde{k}_a$ is assumed to be 1.8 from Table 1, and Δ_0 to be 1.0 so as to reproduce the x dependence of Q near $T = 0$ K [35]. The life-time Γ is taken to be zero for simplicity. Note that the value of Δ_0 is a little smaller than the value in Table 1 due to the assumption of $\Gamma = 0$. From the fact that the wavenumber of Q_0 approaches 0.28 $[2\pi/c]$ as x tends to zero, E_f/v_1 is estimated to be 0.14 $[2\pi/c]$.

Because the experimental data are so much scattered, we determine two fitting parameters J_0 and B so as to make the calculated magnon-energies provide the fit to the experimental data both at $q_z = Q_0$ and at $q_z = 2\pi/c$. Table 3 shows the values of fitting parameters. The values of B are in good agreement with the value for pure Tb, 0.30 meV, estimated by Kasuya [1]. The values for J_0 do not increase linear but concave as x increases. This fact indicates that the conduction band has not the simplified linear-dispersion of k_z in Eq. (3) but a usual quadratic-dispersion. The reason is that the bottom of the conduction band plays an important role in the case of $\Delta_0 = 1.0$. Note that the same discrepancy is also observed in the temperature dependence of magnon dispersions of helical Ho in Fig. 16. The anomaly of the concentration dependence of the magnon energies which occurs for $q < Q$ described as the feature (c) in Sec. 1 is naturally explained by replacing Δ by $x\Delta_0$, that is, by using the non-linear c-f exchange model as shown in Fig. 17. The calculated dispersions show a softening around $q_z = 0.56$ $[2\pi/d]$ due to the instability of the formation of the second-order harmonic. Actually this instability is observed in the case of $x = 0.1$ while in the other cases smeared by the life-time effect.

Finally, we consider magnon dispersions of conical phase. The most striking feature is that the magnon velocity for $q_z > 0$ is different from one for $q_z < 0$ as shown in